Supplementary information for "Engineering the charge carriers via a two-dimensional heterostructure to enhance the thermoelectric figure of merit"

Guangqian Ding*[ab], Cong Wang[b], Guoying Gao*[b], Kailun Yao[b], Chaochao Dun[c], Chunbao Feng[a], Dengfeng Li*[a] and Gang Zhang*[d]

[a]School of Science, Chongqing University of Posts and Telecommunications, Chongqing, 400065, China.

[b]School of Physics and Wuhan National High Magnetic Field Center, Huazhong University of Science and Technology, Wuhan, 430074, China.

[c]Center for Nanotechnology and Molecular Materials Department of Physics, Wake Forest University, Winston-Salem, NC 27109, USA

[d]Institute of High Performance Computing, A*STAR, Singapore.

Section A: DFT and BTE calculations

The structure optimization and energy band structure are calculated within the framework of density functional theory (DFT) using the projector-augmented-wave (PAW) formalism[1] and the Perdew–Burke–Ernzerhof (PBE)[2] exchange and correlation functional, as implemented in VASP.[3] The plane-wave cutoff is set to 500 eV. During the structure optimization, the reciprocal space is sampled by a 3×11×1 Monkhorst-Pack *k*-meshes, ionic and electronic degrees of freedom are fully relaxed until the forces become smaller than 10^{-3} eV/Å. The convergence criteria of the self-consistent loop is set as 10^{-6} eV. The unite cell parameters parallel and perpendicular to the superlattice period are 13.122 Å and 3.788 Å, respectively. Due to radius mismatch of Zr and Hf atoms, all bond lengths and angles exhibit a small deviation from their bulk equilibrium, as shown in Table S1. After determining the equilibrium structure, we calculate the band structure and density of states with a denser *k*-mesh 7×23×1, since the thermoelectric transport coefficient should be tested to converge until a critical *k*-numbers. In order to obtain accurate band gaps and effective masses, we also take mBJ function into consideration.[4]

We calculate the thermoelectric transport coefficients in the framework of the Boltzmann transport equation (BTE) within the constant relaxation time approximation (CRTA) as implemented in BoltzTraP,[5] which describe the deviation from equilibrium of the carrier occupancies under the action of an external field. In the steady state, they can be written as

$$\vec{v} \cdot \nabla_{\vec{r}} f + \frac{1}{\hbar} \vec{F} \cdot \nabla_{\vec{k}} f = -\frac{f - f_0}{\tau}, \qquad (1)$$

where $\vec{F}$ represents the external forces. The electronic transport coefficients can be derived from

the calculated electronic structure, and the key point is to find so-called transport distribution (TD) by solving BTE, which is expressed as

$$\Xi = \sum_{k} \vec{v}_k \vec{v}_k \tau_k , \tag{2}$$

where $\vec{v}_k$ is group velocity of the carriers with wave vector $\vec{k}$, and τ is the carrier relaxation time. Once the TD is defined, the Seebeck coefficient *S*, electrical conductivity σ and electronic contribution to thermal conductivity κ_e tensors are calculated by

$$\sigma = e^2 \int (-\frac{\partial f_0}{\partial \varepsilon}) \Xi(\varepsilon) d\varepsilon , \tag{3}$$

$$S = \frac{e k_B}{\sigma} \int (-\frac{\partial f_0}{\partial \varepsilon}) \frac{\varepsilon - \mu}{k_B T} \Xi(\varepsilon) d\varepsilon , \tag{4}$$

$$\kappa_e = k_B^2 T \int d\varepsilon (-\frac{\partial f_0}{\partial \varepsilon}) \left(\frac{\varepsilon - \mu}{k_B T} \right)^2 \Xi(\varepsilon) , \tag{5}$$

where μ and f_0 are the chemical potential and equilibrium Fermi function, respectively.[6] The calculation of TD are carried out in the subroutine DOS and are output to the file case.sigxx in. Within CRAT, S can be directly evaluated from band structure, while the evaluation of σ and κ_e require the knowledge of τ, which is usually taken from experiment or estimated via deformation potential theory.

Table S1. Comparison of bond lengths and angles between SLM and bulk components. Due to radius mismatch of Zr and Hf atoms, all bond lengths and angles exhibit a small deviation from their bulk equilibrium.

Bond	*d* (Å)	Angle	θ (degree)

SLM	Hf-Se1	2.682	Se1-Hf-Se2	90.621
	Hf-Se2	2.686	Se2-Hf-Se3	90.253
	Hf-Se3	2.683	Se3-Hf-Se4	91.317
	Hf-Se4	2.679		
	Ze-Se1	2.705	Se1-Zr-Se2	90.813
	Zr-Se2	2.709	Se1-Zr-Se4	91.173
	Zr-Se3	2.711	Se3-Zr-Se4	90.1
	Zr-Se4	2.707		
Bulk-$ZrSe_2$	Zr-Se	2.67	Se-Zr-Se	89.839[7]
Bulk-$HfSe_2$	Hf-Se	2.675	Se-Hf-Se	90.153[7]

The lattice thermal conductivity is calculated by phonon Boltzmann transport equation (pBTE) as implemented in ShengBTE.[8] When considering two- and three-phonon process as the scattering sources, the linearized pBTE is written as: $\vec{F}_\lambda = \tau_\lambda^0(\vec{v}_\lambda + \Delta_\lambda)$, where $\vec{v}_\lambda$ is the group velocity of mode λ, τ_λ^0 is the relaxation time of mode λ, and Δ_λ in the dimension of velocity is a correction of deviation to RTA prediction. If Δ_λ is set to zero, the calculation is equivalent to working within the RTA. Δ_λ and τ_λ^0 are individually calculated as

$$\begin{aligned}\Delta_\lambda = &\frac{1}{Z}\sum_{\lambda'\lambda''}^{+}\Gamma^{+}_{\lambda\lambda'\lambda''}(\zeta_{\lambda\lambda''}F_{\lambda''} - \zeta_{\lambda\lambda'}F_{\lambda'}) \\ &+\frac{1}{Z}\sum_{\lambda'\lambda''}^{-}\frac{1}{2}\Gamma^{-}_{\lambda\lambda'\lambda''}(\zeta_{\lambda\lambda''}F_{\lambda''} + \zeta_{\lambda\lambda'}F_{\lambda'}) + \frac{1}{Z}\sum_{\lambda'}\Gamma_{\lambda\lambda'}\zeta_{\lambda\lambda'}F_{\lambda'}\end{aligned} \tag{6}$$

$$\frac{1}{\tau_\lambda^0} = \frac{1}{Z}\left(\sum_{\lambda'\lambda''}^{+}\Gamma^{+}_{\lambda\lambda'\lambda''} + \sum_{\lambda'\lambda''}^{-}\frac{1}{2}\Gamma^{-}_{\lambda\lambda'\lambda''} + \sum_{\lambda'}\Gamma_{\lambda\lambda'}\right) \tag{7}$$

The quantities $\Gamma^{\pm}_{\lambda\lambda'\lambda''}$ are the three-phonon scattering rates and $\Gamma_{\lambda\lambda'}$ is the scattering probabilities from isotopic disorder. The lattice thermal conductivity can be finally calculated in term of $\vec{F}_{\lambda}$ as

$$\kappa_l^{\alpha\beta} = \frac{1}{k_B T^2 \Omega N} \sum_{\lambda} f_0(f_0+1)(\hbar\omega_\lambda)^2 \upsilon_\lambda^\alpha F_\lambda^\beta \qquad (8)$$

A full solution of pBTE requires inputs including descriptions of the harmonic and anharmonic interatomic force constants (IFCs) in the crystal structure. We employ VASP to calculate the IFCs using a well-converged 2×5×1 supercells based on the relaxed unit cell. For the anharmonic IFCs, we impose a converged cutoff distance 0.6 nm for the atomic interactions. The harmonic IFCs are obtained by Phonopy code.[9] For obtaining anharmonic IFCs and for solving pBTE, we employ the ShengBTE code, based on adaptive smearing approach to the conservation of energy and on an iterative solution method.

Section B: Electrical thermal conductivity

The electrical thermal conductivity κ_e is calculated by Wiedemann-Franz law: $\kappa_e = L\sigma T$, where L is the lorentz number, σ the electrical conductivity, and T the absolute temperature. Thus, κ_e is in fact proportional to σ. It is important to emphasize that the lorentz number L plays a critical role in predicting ZT. The value of L for calculating κ_e depends on the type of the semiconductor. For a non-degenerate semiconductor, the lorentz number L is approximately 1.5×10^{-8} V^2K^{-2}.[10] For a degenerate semiconductor, L is obtained as[5]

$$L = \frac{\pi^2}{3}\left(\frac{k_B}{e}\right)^2, \tag{9}$$

which equal to the value of 2.44×10^{-8} V^2K^{-2}.[11] Calculated κ_e for the degenerate SLM at room temperature is shown in Figure S1.

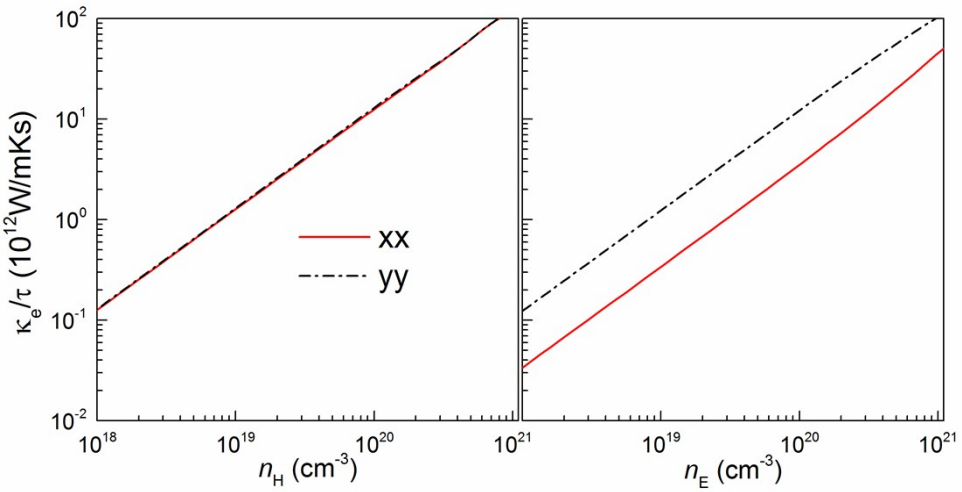

Fig. S1. Electrical thermal conductivity parallel (*x*-axis) and perpendicular (*y*-axis) to the superlattice period at room temperature (300 K).

As shown in Figure S1, κ_e shows similar trend to σ due to their proportional relation. The lower κ_e of electrons along *x*-axis, along with the lower κ_l, contribute to the higher *n*-type *ZT* in this direction.

Section C: DP calculations

As discussed in section A, to evaluate *ZT* still requires the knowledge of carrier relaxation time τ. Here, we adopt the deformation potential (DP) theory based on effective mass approximation to calculate τ.[12,13] For two-dimensional systems, the carrier mobility is calculated as[13]

$$\mu = \frac{e\hbar^3 C_{2D}}{k_B T m^* m_d^* E_l^2}, \tag{10}$$

where C_{2D} is elastic modulus and can be determined by $C_{2D} = \frac{1}{S_0}\frac{\partial^2 E}{\partial(\Delta l / l_0)^2}$, a second order of the total energy with respect to deformation $\Delta l / l_0$, and S_0 is the area of the unit cell. The factor E_l is DP constant, which is calculated as $E_l = \frac{\partial E_{edge}}{\partial(\Delta l / l_0)}$, the slop of the energies at the valence or conduction edges as a function of $\Delta l / l_0$. m^* is the carrier effective mass along transport direction, and m_d^* is the average effective mass and defined by $m_d^* = \sqrt{m_x^* m_y^*}$. Figure S2 shows the normalized energies of band edges and total energy with respect to deformation $\Delta l / l_0$. After all parameters obtained, the relaxation time is defined by

$$\tau = \frac{\mu m^*}{e}, \tag{11}$$

calculated results are listed in Table S2.

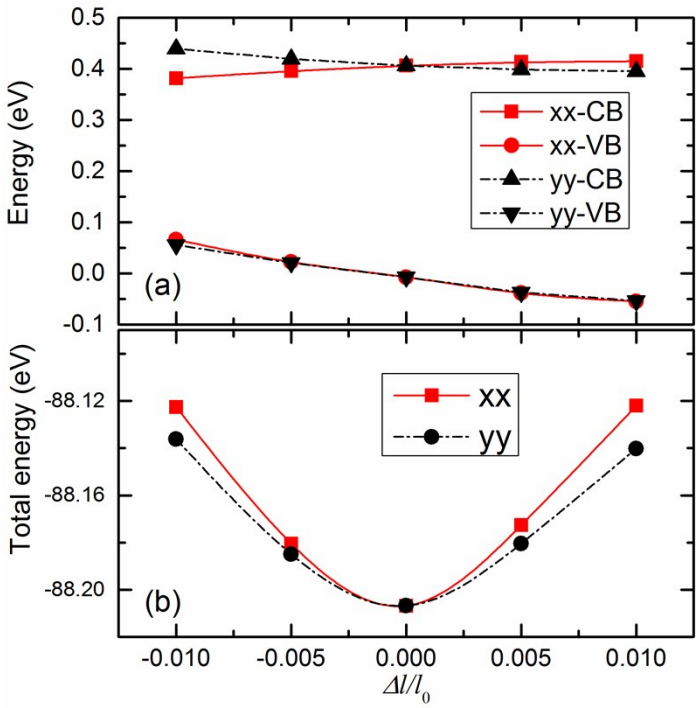

Fig. S2. (a) Energies of the conduction and valence band edges as a function of deformation $\Delta l / l_0$, note that the Fermi energies are normalized by a constant value, which doesn't matter when fitting the slop. (b) The total energies of the unit cell as a function of deformation.

Table S2. DP constant, elastic modulus, effective mass, average effective mass, carrier mobility, and carrier relaxation time at 300 K. Both *n*- and *p*-type along different directions are presented, which are obtained from the primary bands nearing the Fermi level for holes and electrons transport.

	E_l (eV)	C_{2D} (eVÅ^{-2})	m^* (m_e)	m_d^* (m_e)	μ (m^{2}V^{-1}s^{-1})	τ (ps)

xx	*n*	1.68	30.79	4.06	1.22	0.075	1.7
	p	-6.06	30.79	-0.137	0.135	1.549	1.2
yy	*n*	-2.17	24.9	0.369	1.22	0.401	0.84
	p	-5.54	24.9	-0.134	0.135	1.532	1.16

Section D: The formation energy

The formation energy of the superlattice can be quantitatively described by:

$$E_{form}=E(A/B)-aE(A)-bE(B),$$

where a and b are the number of unit cell A and B contained in the SLM structure, respectively. As shown in Table S3, the formation energy in $ZrSe_2/HfSe_2$ superlattice is -0.1723 eV per unit cell, comparable with that in $MoS_2/MoSe_2$ superlattice. Considering the experimental synthesis of $MoS_2/MoSe_2$ superlattice,[14,15] the $ZrSe_2/HfSe_2$ superlattice structure is also expected to be realizable experimentally.

Table S3. Formation energy of $ZrSe_2/HfSe_2$ and $MoS_2/MoSe_2$ SLM.

	$ZrSe_2$	$HfSe_2$	$ZrSe_2/HfSe_2$ SLM	E_{form}
Energy (eV/unit cell)	-1805.2839	-932.8169	-5476.3739	-0.1723
	MoS_2	$MoSe_2$	$MoS_2/MoSe_2$ SLM	E_{form}
Energy (eV/unit cell)	-2495.4495	-2458.8045	-4954.5674	-0.3134

Section E: Supporting figures

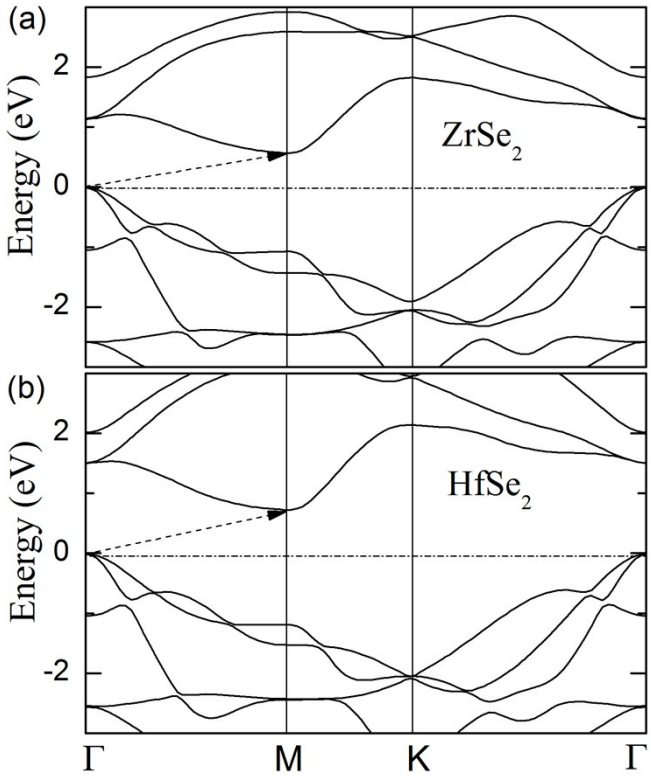

Fig. S3. Band structures of $ZrSe_2$ (a) and $HfSe_2$ (b) monolayers.

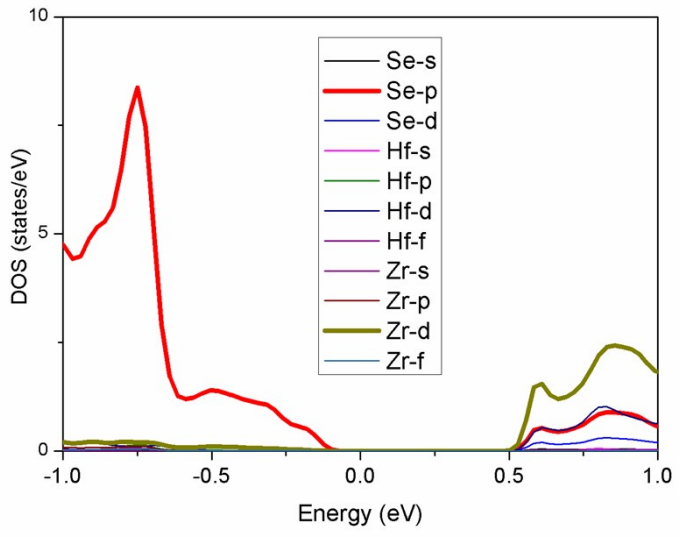

Fig. S4 Partial density of states of the $ZrSe_2/HfSe_2$ SLM.

References

1 P. E. Blöchl, *Phys. Rev. B.,* 1994, **50**, 17953-17979.

2 J. P. Perdew, K. Burke and M. Ernzerhof, *Phys. Rev. Lett.,* 1996, **77**, 3865-3868.

3 G. Kresse and J. Furthmüller, *Phys. Rev. B*., 1996, **54**, 11169-11186.

4 F. Tran and P. Blaha, *Phys. Rev. Lett.,* 2009, **102**, 226401.

5 G. K. H. Madsen and D. J. Singh, *Comput. Phys. Commun.,* 2006, **175**, 67-71.

6 T. J. Scheidemantel, C. Ambrosch-Draxl, T. Thonhauser, J. V. Badding and J. O. Sofo, *Phys. Rev. B.,* 2003, **68**, 125210.

7 R. M. A. Lieth and J. C. J. M. Terhell, Springer: Berlin, 1977, pp 141-223.

8 W. Li, J. Carrete, N. A. Katcho and N. Mingo, *Comput. Phys. Commun.,* 2014, **185**, 1747-1758.

9 A. Togo, F. Oba and I. Tanaka, *Phys. Rev. B.,* 2008, **78**, 134106.

10 R. Venkatasubramanian, E. Siivola, T. Colpitts and B. O'Quinn, *Nature*., 2001, **413**, 597-602.

11 G. J. Snyder and E. Toberer, *Nat. Mater.,* 2008, **7**, 105-114.

12 J. Bardeen and W. Shockley, *Phys. Rev.,* 1950, **80**, 72−80.

13 L. C. Zhang, G. Qin, W. Z. Fang, H. J. Cui, Q. R. Zheng, Q. B. Yan and G. Su, *Sci. Rep.,* 2016, **6**, 19830.

14 X. Duan. *et al Nat. Nanotechnol.*, 2014, **9**, 1024.

15 K. Chiu, K. Huang, C. Chen, Y. Lai, X. Zhang, E. Lin, M. Chuang, J. Wu and Y. Lee, *Adv. Mater.* 2018, **30**, 1704796.